

Laser Probe for the Detection of Surface Acoustic Waves

by

Emory Albers

A PROJECT

submitted to

Oregon State University

University Honor's College

in partial fulfillment of  
the requirements for the  
degree of

Honors Baccalaureate of Science in Electrical Engineering (Honor's Scholar)

Presented May 30, 2007  
Commencement June 2007

## AN ABSTRACT OF THE THESIS OF

Emory Albers for the degree of Honors Baccalaureate of Science in Electrical Engineering presented on May 30, 2007. Title: Laser Probe for the Detection of Surface Acoustic Waves.

Abstract approved:

---

Pallavi Dhagat

The amplitude and phase of surface acoustic waves can be characterized using a laser beam and photodiode detector. This paper describes a technique for characterizing waves using the double photodiode method. This method is a modification of the knife-edge method, and involves focusing a laser beam to a beam spot smaller than the acoustic wavelength. The beam is reflected and the tilt of the reflection due to the surface acoustic wave is measured by a double photodiode. The laser beam is chopped to the same frequency as the surface acoustic wave and amplitude modulation is applied in order for the photodiode to be able to detect the wave. The double photodiode measures the light shining on each half of the detector. The difference between signals from each half is then divided by the total signal and fed into a lock-in amplifier that extracts the amplitude and phase information from the signal. The lock-in amplifier output signal can also be used to create 2D images of the surface acoustic wave using LabView or another similar program. The described method has been shown to be applicable to frequencies of 3 GHz and will have a measured amplitude sensitivity of 1 angstrom.

Key Words: Surface acoustic wave, SAW, laser probe, double photodiode method

Corresponding e-mail address: [alberse@engr.orst.edu](mailto:alberse@engr.orst.edu)

©Copyright by Emory Albers  
May 30, 2007  
All Rights Reserved

Laser Probe for the Detection of Surface Acoustic Waves

by

Emory Albers

A PROJECT

submitted to

Oregon State University

University Honor's College

in partial fulfillment of  
the requirements for the  
degree of

Honors Baccalaureate of Science in Electrical Engineering (Honor's Scholar)

Presented May 30, 2007  
Commencement June 2007



Honors Baccalaureate of Science in Electrical Engineering project of Emory Albers  
presented on May 30, 2007.

APPROVED:

---

Mentor, representing Electrical Engineering – Materials and Devices

---

Committee Member, representing Electrical Engineering – Materials and Devices

---

Committee Member, representing Electrical Engineering – Materials and Devices

---

Dean, University Honors College

I understand that my project will become part of the permanent collection of Oregon State University, University Honors College. My signature below authorizes release of my project to any reader upon request.

---

Emory Albers, Author

## **ACKNOWLEDGEMENTS**

I would like to acknowledge and thank Dr. Pallavi Dhagat for inviting me to join her research group, for proposing this project and for all her guidance along the way as my mentor. I would like to thank Dr. Tom Plant for sharing his knowledge on lasers and detectors and for allowing me to borrow equipment to complete my project. I would also like to thank Dr. Albrecht Jander for all of his contributions, especially in the area of op-amps. Without the help of the above professors, this project would have been difficult to complete.

## TABLE OF CONTENTS

	<u>Page</u>
1. INTRODUCTION .....	1
2. SURFACE ACOUSTIC WAVES .....	2
3. INSTRUMENT DESIGN .....	3
3.1 THE LASER AND LENS.....	3
3.2 KNIFE-EDGE METHOD .....	7
3.3 DOUBLE PHOTODIODE METHOD .....	8
3.3.1 PIN PHOTODIODE DETECTOR BASICS .....	8
3.3.2 DOUBLE PHOTODIODE .....	10
3.4 DETECTION CIRCUIT .....	11
3.5 MODULATION AND THE STOBOSCOPE EFFECT .....	15
3.5.1 ELECTR-OPTIC MODULATION AND THE STROBOSCOPE EFFECT .....	15
3.5.2 AMPLITUDE MODULATION .....	15
3.6 SAMPLE SCANNING .....	16
4. SIGNAL PROCESSING .....	17
4.1 THE DETECTED SIGNAL .....	17
4.2 LOCK-IN AMPLIFIER .....	18
4.3 SIGNAL IMAGING .....	19
5. RESULTS .....	21
5.1 DETECTOR CIRCUIT CHARACTERIZATION .....	21
5.2 NOISE CALCULATIONS .....	25
6. CONCLUSIONS .....	28
REFERENCES .....	29
APPENDIX: MATLAB SCRIPTS .....	30

## LIST OF FIGURES

	<u>Page</u>
FIGURE 1: INTERDIGITATED TRANSDUCERS USED TO EXCITE SURFACE ACOUSTIC WAVES .....	2
FIGURE 2: SURFACE ACOUSTIC WAVE .....	2
FIGURE 3: INSTRUMENT SET UP .....	3
FIGURE 4: FOCUSING LENS ARRANGEMENT .....	4
FIGURE 5: GRAPH SHOING FOCAL LENGTH VS. FOCUSED BEAM DIAMETER.....	5
FIGURE 6: TELESCOPING LENS ARRANGEMENTS .....	6
FIGURE 7: GRAPH SHOWING INPUT BEAM VS. FOCUSED BEAM DIAMETER .....	6
FIGURE 8: KNIFE-EDGE SET UP .....	7
FIGURE 9: PIN PHOTODIODE LAYOUT AND DIMENSIONS .....	8
FIGURE 10: PIN JUNCTION DIODE WITH DEPLETION REGION .....	9
FIGURE 11: DOUBLE PHOTODIODE SET UP .....	10
FIGURE 12: DETECTION CIRCUIT SCHEMATIC .....	12
FIGURE 13: OP AMP CURRENT TO VOLTAGE CONVERTER .....	13
FIGURE 14: OP AMP DIFFERENCE AMPLIFIER .....	13
FIGURE 15: OP AMP SUMMING AMPLIFIER .....	14
FIGURE 16: DIVIDER SET UP .....	14
FIGURE 17: AMPLITUDE MODULATION .....	16
FIGURE 18: PHASE DIFFERENCE .....	18

## LIST OF FIGURES (CONTINUED)

FIGURE 19: AMPLITUDE AND PHASE .....	19
FIGURE 20: DETECTOR CIRCUIT CHARACTERIZATION .....	21
FIGURE 21: MEASURED A+B PHOTODIODE SIGNAL VS. POSITION .....	22
FIGURE 22: MEASURED C+D PHOTODIODE SIGNAL VS. POSITION .....	23
FIGURE 23: MEASURED AND CALCULATED DIFFERENCE SIGNAL VS. POSITION .....	23
FIGURE 24: MEASURED AND CALCULATED SUM SIGNAL VS. POSITION .....	24
FIGURE 25: MEASURED AND CALCULATED DIVIDER SIGNAL VS. POSITION .....	25

## LIST OF TABLES

	<u>Page</u>
TABLE 1: DETECTION CIRCUIT COMPONENT VALUES .....	12
TABLE 2: DETECTOR CIRCUIT OP AMP CHARACTERIZATION .....	22
TABLE 3: DIVIDER CHARACTERIZATION .....	25
TABLE 4: RESISTOR NOISE CALCULATIONS .....	27

## Laser Probe for the Detection of Surface Acoustic Waves

### 1. Introduction

The purpose of this thesis project was to explore and develop a way to characterize surface acoustic waves using a laser. The OSU Applied Magnetics Lab is currently conducting research on using surface acoustic wave devices for magnetic field sensor applications. In addition to being used for sensing, the devices will be remotely interrogable to enable wireless sensor networks. In order to support the research, a way to determine the amplitude and phase of a surface acoustic wave must be developed, as well as the ability to graphically image the wave.

Presently there are no commercial systems available to image surface acoustic waves. Several universities and research labs have published papers detailing their techniques to image the waves. The proposed design was determined after a review of the available literature and chosen for its simple optical set-up, potential for sensitivity of about 1 angstrom and applicability to surface acoustic waves in the gigahertz frequency.

## 2. Surface Acoustic Waves

Surface acoustic waves (SAW) are mechanical stress waves that propagate on top of or close to the surface of a material. The waves can be excited on a piezoelectric material using interdigitated transducers (IDTs), as seen in Figure 1. The metal fingers of the IDT set up an electric field in the material causing it to contract or expand along the surface (Figure 2) [1].

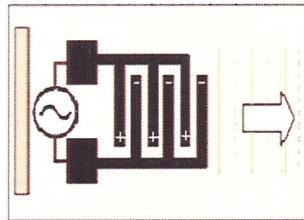


**Figure 1: Interdigitated transducers used to excite surface acoustic waves**

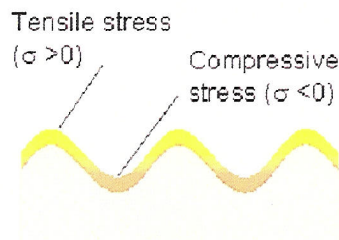


**Figure 2: Surface acoustic wave**

SAW devices can be used as sensors, filters, oscillators and transformers. Currently, SAW filters are widely used in cellular phones due to the size, performance and cost benefits [1].



### 3. Instrument Design

An overview of the instrument design can be seen in Figure 3. In this section and the next, the design will be dissected into its individual components and discussed in detail. This instrument design is based on Engan's [2], which was reported to be capable of measuring the phase and amplitude of surface acoustic waves and is expected to be useful up to 3 GHz.

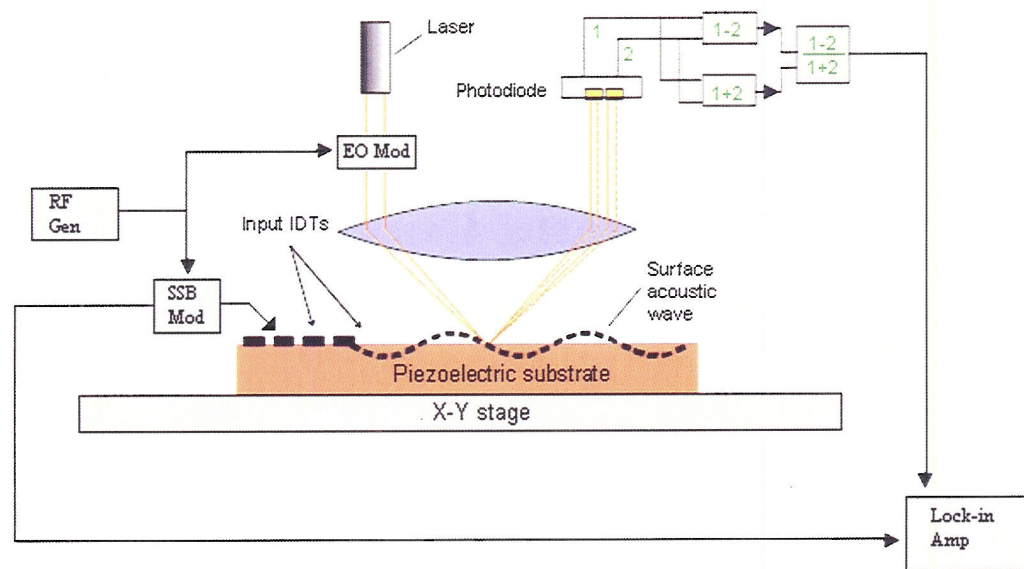


**Figure 3: Instrument set up**

#### 3.1 The Laser and Lens

The laser chosen for the instrument is a helium neon (HeNe) laser. The HeNe laser was chosen based on its availability and because it outputs a visible red light that makes alignment much easier (as opposed to a laser operating outside of the visible spectrum). The laser outputs light of wavelength  $\lambda = 632.8 \text{ nm}$  and has a Gaussian beam diameter of about 2 mm.

In order to image a surface acoustic wave, the laser beam must be focused to a spot size that is at least half of the acoustic wavelength [2]. The wavelength of the SAW currently being induced in the devices under research is about 40  $\mu\text{m}$ , which means the beam needs to be focused to a spot smaller than 20  $\mu\text{m}$ .

A bi-convex lens was used to focus the beam. The setup for the laser and lens can be seen in Figure 4. The diffraction limited theory (Equation 1) was used to determine the focal length ( $f$ ) of the lens needed. The input beam radius is denoted by  $\omega_{in}$ , (diameter equal to  $2\omega_{in}$ , as shown in Figure 4), and the output beam radius is  $\omega_{out}$ . In this equation,  $n$  is the index of refraction and is equal to one since the beam is propagating through the air [3].

$$\omega_{out} = 1.22 \frac{\lambda f}{2n\omega_{in}} \quad (1)$$

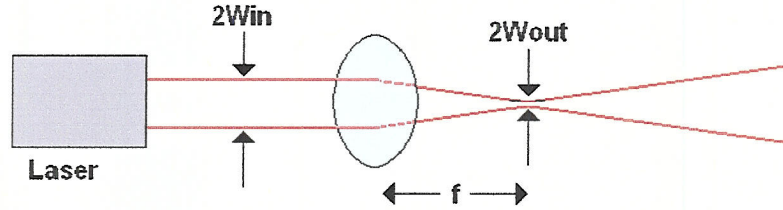


**Figure 4: Focusing lens arrangement**

A Matlab script was written (see Appendix) to determine the focused beam diameter vs. the focal length lens, using the diffraction limited theory. The resulting graph can be seen in Figure 5, and the focal length of the lens was chosen to be 12 mm, in order to allow for slightly more room for the beam to pass through the lens twice (the incident and reflected beams). The lens was purchased from Edmund Optics (part

number NT47-358) and has an antireflection coating applied to reduce surface reflections and thereby increase transmission. A lens holder was purchased from Newport (part number LH-0.5).

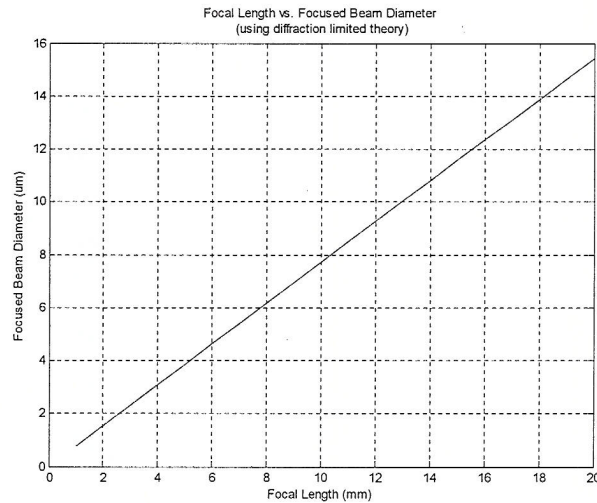


**Figure 5: Graph showing focal length vs. focused beam diameter**

In the future, if smaller wavelength SAWs are needed to be imaged the lens setup can be modified to accommodate them. Two lenses can be added between the laser and the focusing lens in a telescoping set up, as seen in Figure 6a and 6b. By increasing the input beam diameter to the focusing lens, the beam can be focused to a smaller spot [3]. A Matlab script was written (see Appendix) to show the relationship between input beam diameter and focused beam diameter. The results can be seen in Figure 7.

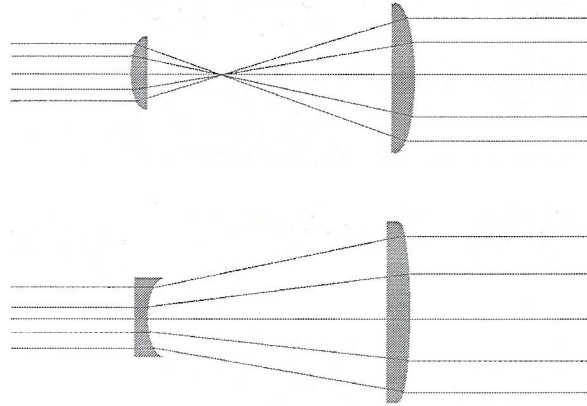


**Figure 6: Telescoping lens arrangements, (a) Keplerian, (b) Galilean**

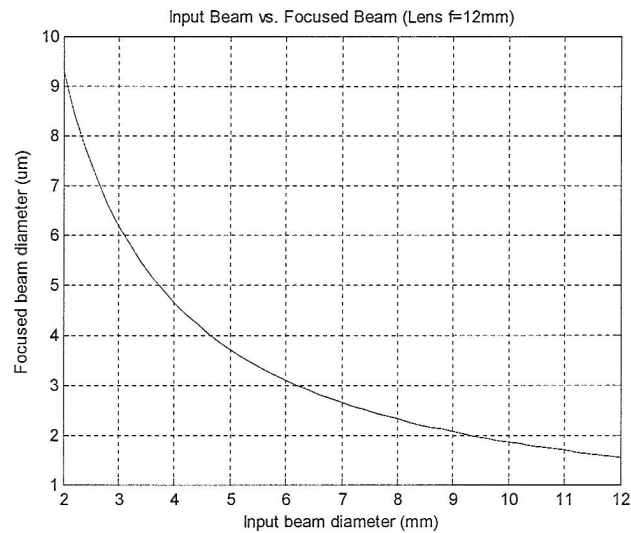


**Figure 7: Graph showing input beam vs. focused beam diameter**

There are two types of telescope lens arrangements that can be used, the Keplerian and the Galilean. In the Keplerian arrangement, two positive lenses are used and the arrangement has a real focal length in between the lenses [3], as seen in Figure 6a. The Galilean arrangement uses one positive and one negative lens, and thus has no focal point [3], as seen in Figure 6b. In both arrangements, the system will act as a beam

expander if the distance between the two lenses ( $d$ ) is equal to the sum of the two focal lengths of the lenses ( $f_1$  and  $f_2$ ) [3].

$$d = f_1 + f_2 \quad (2)$$

The magnification of the system will be equal to the division of the focal lengths [3]:

$$M_{lens} = \frac{-f_2}{f_1} \quad (3)$$

When applying a telescoping arrangement to the current laser and lens system, care must be taken to keep the input beam diameter small enough to allow room for the beam to pass through the lens twice.

### 3.2 Knife-Edge Method

One possible method for detecting the displacement of the laser beam due to the surface acoustic wave is the knife-edge method. The method is discussed by Alder et al [4] and Rostad [1]. The knife-edge obstructs part of the reflected beam (see Figure 8) and the photodiode detector generates a signal that is at the same frequency as the surface wave. The signal contains phase and amplitude information that can be extracted.

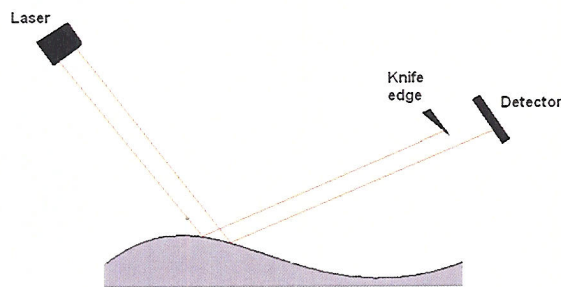


Figure 8: Knife-edge set up



### 3.3 Double Photodiode Method

Due to the complexity of alignment inherent with the knife-edge method, the double photodiode method was chosen. The double photodiode method also offers advantages in detection frequency; it has been reported by Engan [2] to be applicable to SAW frequencies up to 3GHz, while the knife-edge method has not been reported to work at frequencies higher than a few tens of MHz [2].

Photodiodes can be purchased in double and quad packages (quads are most popular) that contain separate active areas, each with their own output, separated by a small distance from each other, as seen in Figure 9. For this project a PIN junction photodiode with the dimensions shown in Figure 9 was used. Before going into more detail about the photodiode used, the basic operation of a PIN photodiode detector should be covered.

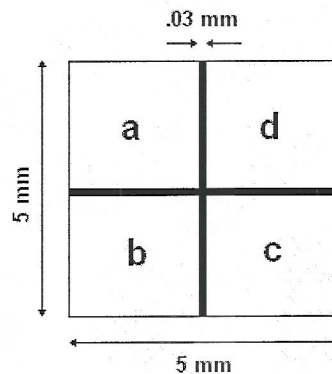


**Figure 9: PIN photodiode layout and dimensions**

#### 3.3.1 PIN Photodiode Detector Basics

The operation of a PIN photodiode can be explained by first examining a PN junction photodiode. A PN photodiode is created when an n-type material is connected to a p-type material. The electrons from the n-type material diffuse into the p-type material and recombine, while the holes from the p-type material do the same with the n-

type material [3]. This creates a depletion region in the center where no free charges exist, that is bordered by positive ions on the n-side and negative ions on the p-side [3]. Therefore, when free charges enter the depletion region they are swept to one side or the other by the field produced by the ions (electrons to the n-side and holes to the p-side) [3].

When light is incident on the detector, an electron-hole pair is created and each is swept to their respective side [3]. This creates a photocurrent as long as the light is incident within about one diffusion length of the depletion region [3]. If the carriers are created too far from the depletion region they will recombine [3].

In order to increase the quantity of light absorbed by the detector an intrinsic region can be added between the n and p regions, see Figure 10. This intrinsic layer makes the depletion region larger, which allows more optical carriers to be created. The response time for the detector is limited by the carrier transit time through the depletion layer [3]. The region is usually kept a thickness of  $1/\alpha$ , where  $\alpha$  [units of distance<sup>-1</sup>] is the optical absorption at a certain wavelength of light [3].

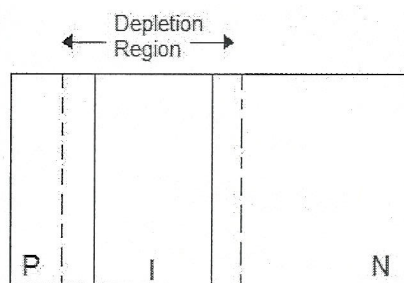


**Figure 10: PIN junction diode with depletion region**

PN and PIN photodiodes can be operated in the photovoltaic, photoconductive or open-circuit mode. In the photovoltaic mode, the diode is forward biased by a positive voltage applied to the p-side. This mode is used when dynamic range is important [3]. In

the photoconductive mode the diode is reverse biased by a positive voltage applied to the n-side. This is useful when response speed and linearity are important [3]. In the open-circuit mode no net current is produced because the light induced carrier current is balanced by a diffusion current in the opposite direction [3].

### 3.3.2 Double Photodiode

The set-up for the double photodiode method can be seen in Figure 11. The laser beam is focused through a lens onto the surface acoustic wave and then reflected back through the lens to its original beam shape. This set-up transforms the displacement in angle from the SAW reflection to a horizontal displacement on the photodiode detector [2]. The detector is arranged to measure the difference in output between its two horizontal halves. The detector is aligned so that in the absence of an acoustic wave the reflected beam is centered on the detector and the output is zero [2].

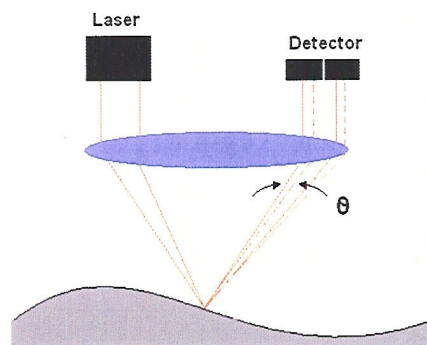


**Figure 11: Double photodiode set up**

When a wave is present, the reflected beam is displaced from the center and the difference from the two halves of the detector is nonzero. The output signal from each half of the detector is put through a detection circuit, discussed in 3.4, which takes the difference of the signals as well as summing the two signals. The difference signal



changes with the position of the surface acoustic wave, by angle  $\theta$ , while the sum of the two signals remains the same. The difference signal is normalized by the summing signal and the final result is a harmonically varying voltage signal [2].

For this project, a Hamamatsu S7479 quad PIN photodiode was used. Since detection is only needed in one plane, two quadrants are tied together to essentially make the photodiode a double photodiode that detects displacement in one direction.

The Hamamatsu photodiode has a sensitivity that varies with wavelength. The optimum sensitivity of .72 is obtained when the diode is detecting light of wavelength 960 nm. For the current arrangement, the photodiode is detecting the HeNe laser source at a wavelength of 632.8 nm, so the device has a sensitivity of about 0.42 A/W, as determined from its datasheet [5]. This reduced sensitivity has an effect on the noise level of the photodiode, which is discussed later in Chapter 5.

### **3.4 Detection Circuit**

The detection circuit takes the output signal from each half of the photodiode and translates it into a signal that can be used to determine the amplitude and phase of the detected wave. A schematic of the circuit can be seen in Figure 12, with the associated component values in Table 1. The design of the circuit is a modification of the position calculating circuit from OSI optoelectronics [6], and the National Semiconductor Op Amp Configurations [7] were a great help in designing the circuit. The operation amplifiers used in the circuit are OPA37 and the divider is an AD534.

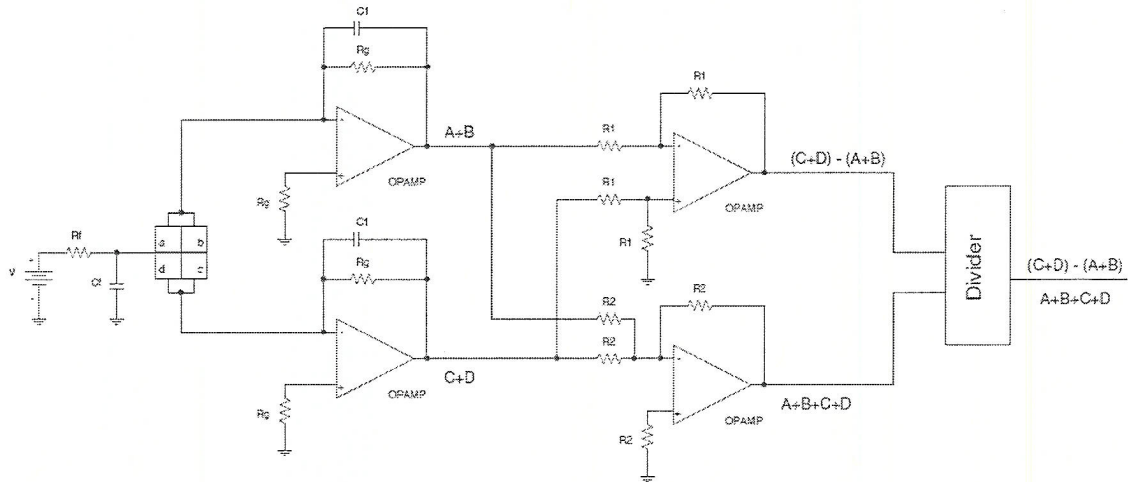


**Figure 12: Detection circuit schematic**

Component	Value	Comments
V	+ 15 V	Reverse bias, 0-20 V
R <sub>f</sub>	9.76 kΩ	
R <sub>g</sub>	1.07 kΩ	Gain resistor
R <sub>1</sub>	191 kΩ	Unity gain, resistor can be any value
R <sub>2</sub>	187 kΩ	Unity gain, resistor can be any value
C <sub>f</sub>	1.5 nF	$C_f = 1/(2\pi R_f f)$
C <sub>1</sub>	1000 pF	

**Table 1: Detection circuit component values**

The photodiode is operating in the photoconductive mode with a positive voltage applied to the cathode (n-side) of the detector. The detector is set-up to measure displacement in only one direction by connecting the output of two segments together and treating them as one signal. Each output from the diode is fed into a current to voltage converter (Figure 13, with pin numbers labeled [8]) that has a gain equal to  $R_g$ :

$$V_{out} = I_{in} R_g \quad (4)$$

The resistor from the positive input to ground was added to decrease the error on the signal due to the bias current of the op amp.

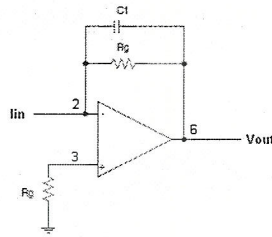


**Figure 13: Op Amp current to voltage converter**

After the current signals from each half of the detector are amplified and converted to voltage signals, the signal difference between the two halves is determined by using a difference amplifier with no gain (see Figure 14). This signal changes with the position of the laser beam. The output signal from this amplifier is:

$$V_{out} = V_2 - V_1 \quad (5)$$

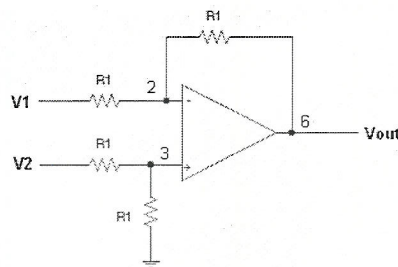


**Figure 14: Op amp difference amplifier**

The amplified voltage signals from each half of the detector are also fed into a summing amplifier (with no gain) to determine the total signal from the light hitting the detector (see Figure 15). This signal will not change as the beam moves across the detector (unless the beam is moved partially off the detector). The output signal from this amplifier is:

$$V_{out} = V_1 + V_2 \quad (6)$$

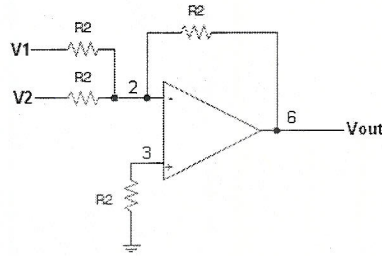


**Figure 15: Op amp summing amplifier**

The difference signal is normalized by dividing it by the total light detected by the photodiode so that it is independent of the optical reflectivity of the film surface. The divider is set up to accept the difference signal as the numerator and the sum signal as the denominator. The divider has an internal gain of 10 V and is capable of adding a signal to the division result. The added signal is not used and therefore grounded as are  $Z_1$  and  $X_2$ . The connections of the divider can be seen in Figure 16 [9]. The output voltage signal is:

$$V_{out} = 10 \frac{Z_2}{X_1} \quad (7)$$

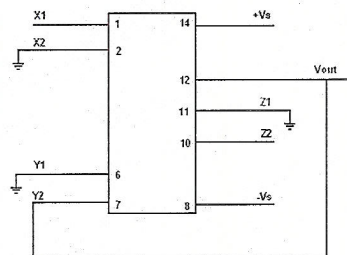


**Figure 16: Divider set up**

Characterization and noise calculations of the detector circuit are discussed in Chapter 5.

### **3.5 Modulation and the Stroboscope Effect**

Saw excitation frequencies are quite high around 100 MHz or greater. Most photodiodes are unable to detect SAW frequencies, and cut off at much lower frequencies. The Hamamatsu photodiode used in this project cuts off around 10-20 MHz [5]. Therefore, modulation must be applied in order for the detector to retrieve the amplitude and phase of the surface acoustic wave.

#### **3.5.1 Electro-Optic Modulation (EO Mod) and the Stroboscope Effect**

The laser beam is chopped at the same frequency as excitation signal to the IDT, by an electro-optic modulator. The effect of this intensity modulation is to “freeze” the motion of the wave [2]. Do to stroboscope effect the waves appear as though they are standing still to the detector. The signal from the detector is therefore a DC signal that changes as the beam is moved across the wave [1]. This modulation alone is not accurate enough, since small deviations from centering the diode can become several magnitudes of order larger, since only a small amount of the light is affected by the wave and the remaining light sees the film surface as a reflective mirror [1].

#### **3.5.2 Amplitude Modulation**

In order to get a more accurate detection of the SAW, amplitude modulation is added to the system. Amplitude modulation is used to mix the high frequency signal down to a lower detectable frequency while still keeping the necessary information [1]. A low signal frequency generated by the single-side-band modulation (SSB – Figure 3) (Figure 17b) is mixed in with the high excitation frequency, generated by the radio



frequency generator (RF Gen – Figure 3), (Figure 17a). The resulting signal on the piezoelectric substrate is the still propagating wave oscillating at a low frequency (Figure 17c) [2]. The amplitude and phase of the excitation signal are maintained. A lock-in amplifier is used to extract the low frequency signal from the photo detector, discussed later in 4.2.

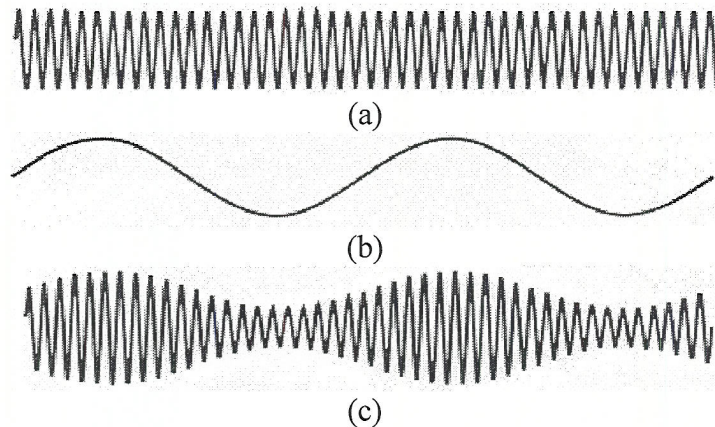


**Figure 17: Amplitude modulation: (a) high frequency signal, (b) low frequency modulation (c) resulting signal**

### 3.6 Sample Scanning

In order to characterize the surface acoustic wave fully, the laser probe must be scanned across the surface of the film [2]. Since moving the entire setup would be difficult, the sample is positioned on a translatable stage. The stage must be capable of precise, computer controlled movements in the X and Y directions.

## 4. Signal Processing

After the surface acoustic wave is detected by the photodiode and run through the detection circuit, the amplitude and phase of the wave can be extracted. A lock-in amplifier is needed isolate the desired frequency of the signal to determine the amplitude and phase. Lab View or another similar program can be used to image the detected wave.

### 4.1 The Detected Signal

The basic operation of the photodiode detector was discussed in section 3.3.1. When light hits the detector, a photodiode current is created [2]:

$$I_d = C_1[I + b\cos(w_r t)][C_2 + C_3 A_{saw} \cos(w_r t - kx + \varphi) \cos(w_l t)] \quad (8)$$

The surface acoustic wave has an amplitude of  $A_{saw}$  and  $\varphi$  is the phase between the wave and the modulation of the beam [2]. The SAW excitation frequency is denoted by  $w_r$  and the amplitude modulating signal is  $w_l$  [2]. In the above equation the constant  $C_1$  depends on the photodiode conversion efficiency and laser beam intensity,  $C_2$  depends on the position of the photodiode (equals zero when the diode is properly centered) and  $C_3$  depends on the beam geometry [2]. The constant  $b$  depends on how well the laser is modulated and  $k$  is the wave is the wave number magnitude [2]. The first bracket of the equation accounts for the effect of the electro-optic modulation of the laser beam and the second bracket describes the distortion of the film due to the wave and its detection by the photodiode [2].

The signal of interest is the low frequency signal, and can be described by [2]:

$$I_{d,l} = \frac{1}{2} b C_1 C_3 A_{saw} \cos(w_l t - kx + \varphi) \quad (9)$$

This equation relates to the fact that with the electro-optic modulation, the laser beam sees a still wave when scanned along the film surface [2]. It is important to note that the detector will not distinguish between waves traveling in opposite directions. Often the detected surface acoustic wave is the superposition of two waves traveling in opposite directions, and the detected signal can be more accurately represented by [2]:

$$I_{d,l} = \frac{1}{2}bC_1C_3[A_{saw,1}\cos(\omega_1t-kx+\phi_1)+A_{saw,2}\cos\{\omega_1t+kx+\phi_2\}] \quad (10)$$

The detected signal is fed into a lock-in amplifier to determine its phase and amplitude. The basic operation of a lock-in amplifier is discussed next.

## 4.2 Lock-In Amplifier

A lock-in amplifier is used to isolate the useful part of the signal detected by the photodiode and determine its amplitude and phase. The amplifier has two inputs, one for the reference signal from the single-side-band (SSB) modulation and the other is the measured signal from the detection circuit, at the same frequency. The two signals are multiplied by the phase-sensitive detector (PSD) of the amplifier [1]. The resulting signal is sinusoidal with twice the frequency of the input and reference signal [1]. The phase difference between the signals can be seen in graphically in the resulting signal in Figure 18a and 18b [1].

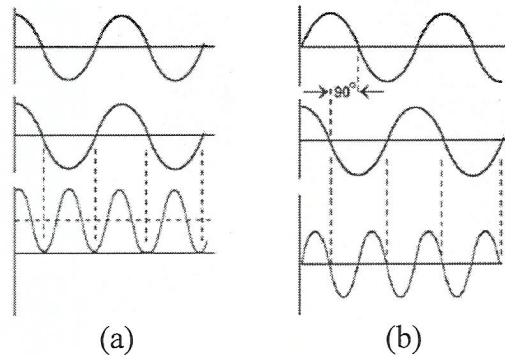


**Figure 18: Phase difference (a) signals in phase, (b) signal 90 degrees out of phase**



Lock-in amplifiers can come as single-phase amplifiers, with one PSD, or dual-phase amplifiers with two PSDs, with the reference signal shifted 90 degrees between the two. Both instrument set-ups can measure the phase and amplitude of the detected signal, but the single-phase amplifier requires two measurements at each point whereas the dual-phase amplifier requires only one measurement. The amplitude and phase can be calculated as follows (as seen in Figure 19) [1]:

$$V_{out} = \sqrt{X^2 + Y^2} \quad (11)$$

$$\theta = \arctan\left(\frac{Y}{X}\right) \quad (12)$$

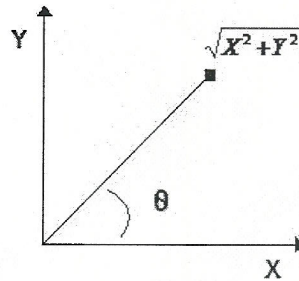


**Figure 19: Amplitude and phase**

In the above equations  $X$  refers to the instrument reading when input and reference signal are taken in phase and  $Y$  refers to the reading when the reference signal is shifted 90 degrees [1]. The dual-phase amplifier takes both of the measurements at the same time, while a single phase amplifier requires that the reference signal be manually shifted 90 degrees (through a knob on the instrument) [1]. The amplitude measurement will remain constant regardless of the changing phase [1].

### 4.3 Signal imaging

After the input and reference signals are fed into the lock-in amplifier, the  $X$  (in phase) and  $Y$  (90 degrees shifted) components can be determined [2]:

$$I_x = \frac{1}{4} b C_1 C_3 \{ A_{SAW,1} \cos(kx - \phi_1 + \phi_r) + A_{SAW,2} \cos(kx + \phi_2 - \phi_r) \} \quad (13)$$

$$I_y = \frac{1}{4} b C_1 C_3 \{ A_{SAW,1} \sin(kx - \phi_1 + \phi_r) - A_{SAW,2} \sin(kx + \phi_2 - \phi_r) \} \quad (14)$$

The shape and period of the above signals are equal to those of the surface acoustic wave, and can be used to image the wave [1]. The amplitude can be calculated by square summing the components above to give:

$$I_A = \frac{1}{4} b C_1 C_3 \{ A_{SAW,1}^2 + A_{SAW,2}^2 + 2 A_{SAW,1} A_{SAW,2} \cos(2kx + \phi_2 - \phi_1) \}^{1/2} \quad (15)$$

Plotting the amplitude signal vs. distance will give the surface acoustic wave pattern.

The maximum values of the plot will be proportional to the sum of the two waves and the minimum values are proportional to the difference between the two waves [2]. The ratio of the two amplitudes can be determined and the phase relation can be determined by the positions of the maxima and minima [2].

## 5. Results

This chapter will discuss the characterization of the detector circuit the noise associated with it.

### 5.1 Detector Circuit Characterization

The detector circuit was characterized using the laser and a fine positioning stage, as shown in Figure 20. The voltage signal after each op amp was measured. The measured difference and sum signals were compared to the calculated signals (from the measured output signal from each half of the photodiode). The error associated with the difference and summing amplifier was determined in volts. All values can be seen below in Table 2.

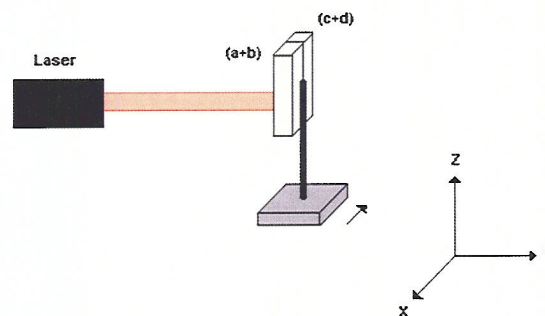


**Figure 20: Detector circuit characterization**

Position (relative)	(A+B) (V)	(C+D) (V)	Difference Amp (V)	Calculated Difference (V)	Error from Calc Diff and Amp (V)	Summing Amp (V)	Calculated Sum (V)	Error between Calc Sum and Amp (V)
-3	-1.98	0.13	2.12	2.11	0.01	1.83	1.85	0.02
-2.5	-1.96	0.11	2.06	2.07	0.01	1.82	1.85	0.03
-2	-1.93	0.09	2.01	2.02	0.01	1.81	1.84	0.03
-1.5	-1.88	0.05	1.94	1.93	0.01	1.8	1.83	0.03
-1	-1.79	-0.02	1.79	1.77	0.02	1.79	1.81	0.02
-0.5	-1.44	-0.33	1.12	1.11	0.01	1.76	1.77	0.01
0	-0.88	-0.88	0	0	0	1.76	1.76	0
0.5	-0.28	-1.51	-1.24	-1.23	0.01	1.76	1.79	0.03
1	-0.05	-1.73	-1.72	-1.68	0.04	1.76	1.78	0.02
1.5	0.03	-1.84	-1.92	-1.87	0.05	1.77	1.81	0.04
2	0.05	-1.88	-1.99	-1.93	0.06	1.77	1.83	0.06
2.5	0.09	-1.9	-2.06	-1.99	0.07	1.77	1.81	0.04
3	0.11	-1.92	-2.08	-2.03	0.05	1.77	1.81	0.04
3.5	0.12	-1.93	-2.12	-2.05	0.07	1.77	1.81	0.04

**Table 2: Detector circuit op amp characterization**

All of the position distances listed above are relative to number of adjustment turns of the translation stage. The amplified signals from each half of the photodiode were plotted and can be seen below in Figures 21 and 22. As expected, the two plots are mirror images of each other, with the large negative signal corresponding to the laser on shining mostly on one half. A small, positive signal is seen when the laser is no longer shining on one half of the detector.

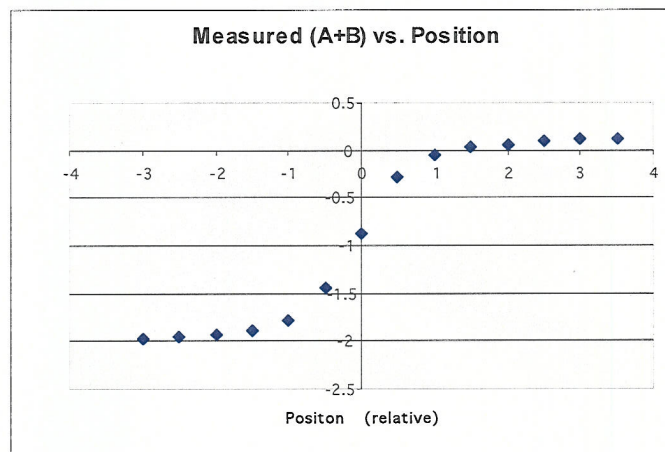


**Figure 21: Measured A+B photodiode signal vs. position**



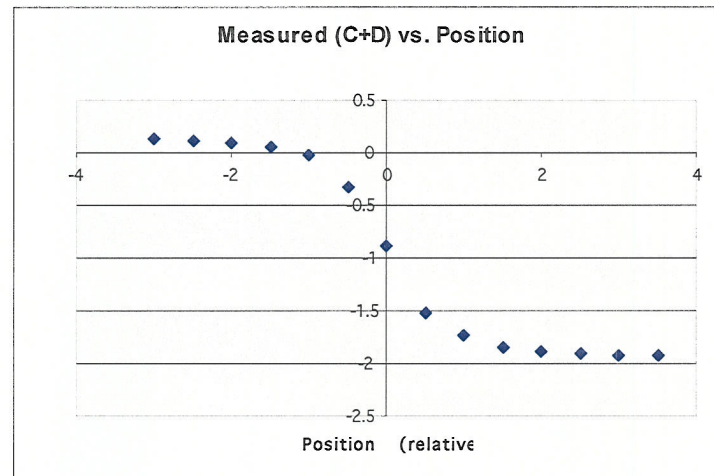


**Figure 22: Measured C+D photodiode signal vs. position**

The measured output from the difference amplifier and the summing amplifier were plotted versus distance along with the calculated values, as seen in Figures 23 and 24. The difference amplifier signal was measured to be quite close to the calculated signal, with a maximum error of 0.07 volts. The measured summing signal and the calculated signal were found to have a maximum error of 0.06 volts.

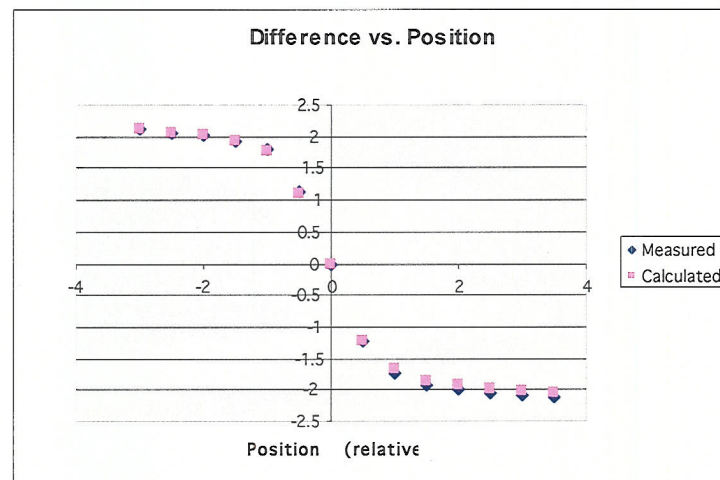


**Figure 23: Measured and calculated difference signal vs. position**

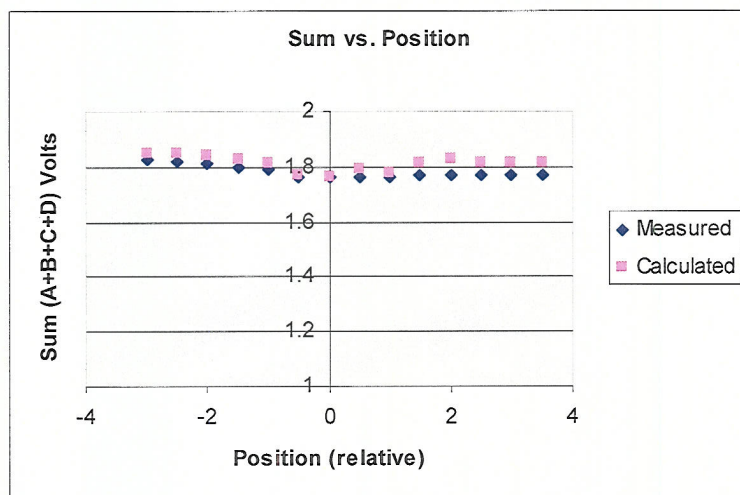


**Figure 24: Measured and calculated sum signal vs. position**

The divider was characterized along with the op amps. The measured value from the divider output was compared to the value calculated by dividing the measured difference signal by the measured summing signal and multiplying by the divider's gain of 10 volts. The error in voltage signal was also calculated. All values can be seen in Table 3. The maximum error was found to be 1.43 volts while the minimum error was 0.02 volts. This wide range in error is undesirable, and cannot be presently explained. The measured and calculated divider signals were plotted and can be seen in Figure 25.

Position (relative)	Difference Amp (V)	Summing Amp (V)	Divider (V)	Calculated Division (V)	Error between Calc Division and Divider (V)
-3	2.12	1.83	10.82	11.58	0.76
-2.5	2.06	1.82	10.52	11.32	0.80
-2	2.01	1.81	10.1	11.10	1.00
-1.5	1.94	1.8	9.35	10.78	1.43
-1	1.79	1.79	8.6	10.00	1.40
-0.5	1.12	1.76	5.43	6.36	0.93
0	0	1.76	-0.61	0.00	0.61
0.5	-1.24	1.76	-7.3	-7.05	0.25
1	-1.72	1.76	-9.85	-9.77	0.08
1.5	-1.92	1.77	-10.88	-10.85	0.03
2	-1.99	1.77	-11.28	-11.24	0.04
2.5	-2.06	1.77	-11.62	-11.64	0.02
3	-2.08	1.77	-11.81	-11.75	0.06
3.5	-2.12	1.77	-12	-11.98	0.02

Table 3: Divider characterization

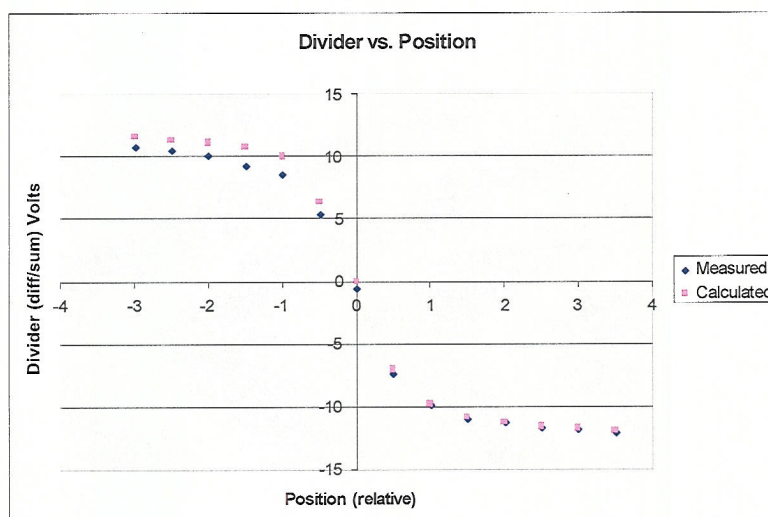


Figure 25: Measured and calculated divider signal vs. position

## 5.2 Noise Calculations

In order to further characterize the detector circuit the noise of the circuit must be calculated in order to determine the signal to noise ratio and the minimum detectable tilt of the surface acoustic wave. The noise for each component must be calculated and then summed together to find the overall noise signal.

In order to determine the noise associated with the photodiode detector the Hamamatsu Photodiode Technical Guide [9] was used. The photodiode noise is the sum of the Johnson noise associated with the shunt resistance of the detector and the shot noise from the dark and light currents.

$$i_{noise} = \sqrt{(i_{Johnson})^2 + (i_{shot,dark})^2 + (i_{shot,light})^2} \quad (16)$$

The Johnson noise can be calculated as follows and dominates in the photovoltaic mode [6]. The constant  $k_B$  is the Boltzman's constant ( $1.38 \times 10^{-23}$  J/K), T refers to the temperature (in Kelvins) and B is the bandwidth (in Hertz).

$$i_{Johnson} = \sqrt{\frac{4k_B T B}{R_{shunt}}} \quad (17)$$

When a bias voltage is applied to the photodiode a dark current is created. The value of the current varies with the amount of bias voltage applied, and was found from the datasheet [5] to be 2.1 nA at a reverse bias of 15 volts. The noise signal associated with the dark current was calculated by the following equation to be  $2.59 \times 10^{-14}$  A/(Hz)<sup>1/2</sup>, per active element, which is insignificant compared to the light current shot noise below.

$$i_{shot,dark} = \sqrt{2qI_D B} \quad (18)$$

A similar equation is used to calculate the shot noise associated with the signal generated by incident light. The maximum value of signal generated by the laser beam was found to be 1.822 mA. The noise signal due to the incident light was calculated to be  $2.415 \times 10^{-11}$  A/(Hz)<sup>1/2</sup>, per 2 elements (A and B tied together as well as C and D).

$$i_{shot,light} = \sqrt{2qI_L B} \quad (19)$$

The total noise was calculated using Equation 16 and found to be  $3.42 \times 10^{-11}$  A/(Hz)<sup>1/2</sup>.



Each resistor in the circuit creates Johnson noise that can be calculated as a current or voltage signal by the following equations. The value of the Johnson noise for each resistor value can be seen in Table 4.

$$i_{Johnson} = \sqrt{\frac{4k_B T B}{R}} \quad (20)$$

$$v_{Johnson} = \sqrt{4k_B T R B} \quad (21)$$

Resistor	Value k $\Omega$	I (Johnson) pA/(Hz) <sup>1/2</sup>	V (Johnson) nV/(Hz) <sup>1/2</sup>
R <sub>f</sub>	9.76	1.3	12.7
R <sub>g</sub>	1.07	3.93	4.21
R <sub>1</sub>	191	0.294	56.24
R <sub>2</sub>	187	0.298	55.65

**Table 4: Resistor noise calculations**

The only Johnson noise that is large enough to have an effect on the total noise of the system is associated with the R<sub>g</sub> resistor; all of the other resistor's Johnson noises can be ignored. The contribution of R<sub>g</sub> to the total noise can be calculated by Equation ## and was found to be  $3.46 \times 10^{-11} \text{ A/(Hz)}^{1/2}$ .

$$i_{noise,total} = \sqrt{2i_{shot,light}^2 + 2i_{Johnson,Rg}^2} \quad (22)$$

The noise equivalent power (NEP) refers to the lower limit of light detection for the photodiode and is expressed as the intensity of incident light required to generate a current signal that is equal to the noise signal. The NEP can be calculated using the following equation and was calculated to be  $8.238 \times 10^{-10} \text{ W/(Hz)}^{1/2}$ . The  $S$  in the equation refers to the sensitivity of the photodiode that was found from the datasheet [5] to be equal to 0.42 A/W.

$$NEP = \frac{i_{noise}}{S} \quad (23)$$

## 6. Conclusions

The purpose of this thesis project was to explore and develop a way to characterize surface acoustic waves using a laser. After a review of the available literature, two dominant methods were evident. The knife edge method, as the name suggests, involves placing a sharp obstacle in the reflected beam path. This method was eliminated due to the extra complexity of aligning an obstacle and the fact that it has not been shown to work at frequencies above a few tens of MHz. The double photodiode method was chosen for this project and is applicable to frequencies up to 3 GHz and has been shown to have a sensitivity around .1 nm.

The instrument design can be seen in Figure 3, and detailed discussions on each component were presented in this paper. Presently, laser has been chosen and a lens selected to focus the beam to a spot size smaller than the acoustic wavelength. The detection circuit has been built and characterized. The error associated with the measured signals has been calculated with a maximum error of 0.07 volts for the op amps and a maximum error of 1.43 volts for the divider.

To complete the instrument, an electro-optic modulator must be purchased that is capable of modulation up to several gigahertz. Currently, the Magnetics Lab has a single phase lock-in amplifier, but to make the SAW characterization easier a second single phase amplifier or a dual phase amplifier will need to be procured. A grant request has been submitted to Physik Instrumente to obtain an X-Y high resolution translation stage.

Once the instrument has been fully assembled, a LabView program can be created to control the instrument, extract the amplitude and phase information and image the wave.

## REFERENCES

- [1] T. Rostad, Optical detection of surface acoustic waves, *Norwegian University of Science and Technology, Department of Electronics and Telecommunications*, 2006.
- [2] H. Engan, Phase sensitive laser probe for high-frequency surface acoustic wave measurements, *IEEE Transactions on Sonics and Ultrasonics*, SU-25, p. 372-377, 1978.
- [3] K.J. Kuhn, *Laser Engineering*, New Jersey: Prentice-Hall, Inc., 1998.
- [4] R. Alder, A. Korpel and P. Desmares, "An instrument for making surface waves visible," *IEEE Transactions on Sonics and Ultrasonics*, vol. SU-15, p. 157-161, 1968.
- [5] Hamamatsu, *Si PIN Photodiode S7479*, 2006.
- [6] OSI Optoelectronics, *Photodiode Characteristics and Applications*.
- [7] National Semiconductor, *Op Amp Circuit Collection*, 1995.
- [8] Analog Devices, *Internally Trimmed Precision IC Multiplier*, 1999.
- [9] Hamamatsu, *Photodiode Technical Guide*.
- [10] Texas Instruments, *Ultra-Low Noise, Precision Operational Amplifiers*, 2005.

## APPENDIX: Matlab Scripts

```
%Determine lens focal length using diffraction theory
lam=632.8e-9;
n=1;
win=1e-3;
f=1e-3:1e-3:20e-3;
wf=1.22*lam*f./(2*n*win);
wfd=2*wf*1e6;
fplot=f.*1e3;
plot(fplot, wfd)
grid on;
xlabel('Focal Length (mm)');
ylabel('Focused Beam Diameter (um)');
title('Focal Length vs. Focused Beam Diameter (using diffraction
limited theory)');
```

```
%Input beam vs. focused beam using diffraction limit Theory
lam = 632.8e-9;
f=12e-3;
n = 1;
win = 1e-3:.1e-3:6e-3;
wf = 1.22*lam*f./(2*n*win);
dia_in = 2*win./1e-3;
dia_out = 2*wf./1e-6;
plot(dia_in, dia_out)
xlabel('Input beam diameter (mm)');
ylabel('Focused beam diameter (um)');
title('Input Beam vs. Focused Beam (Lens f=12mm)');
grid on
```